The Long Island Sound Habitat Mapping Initiative Phase II – Eastern Long Island Sound

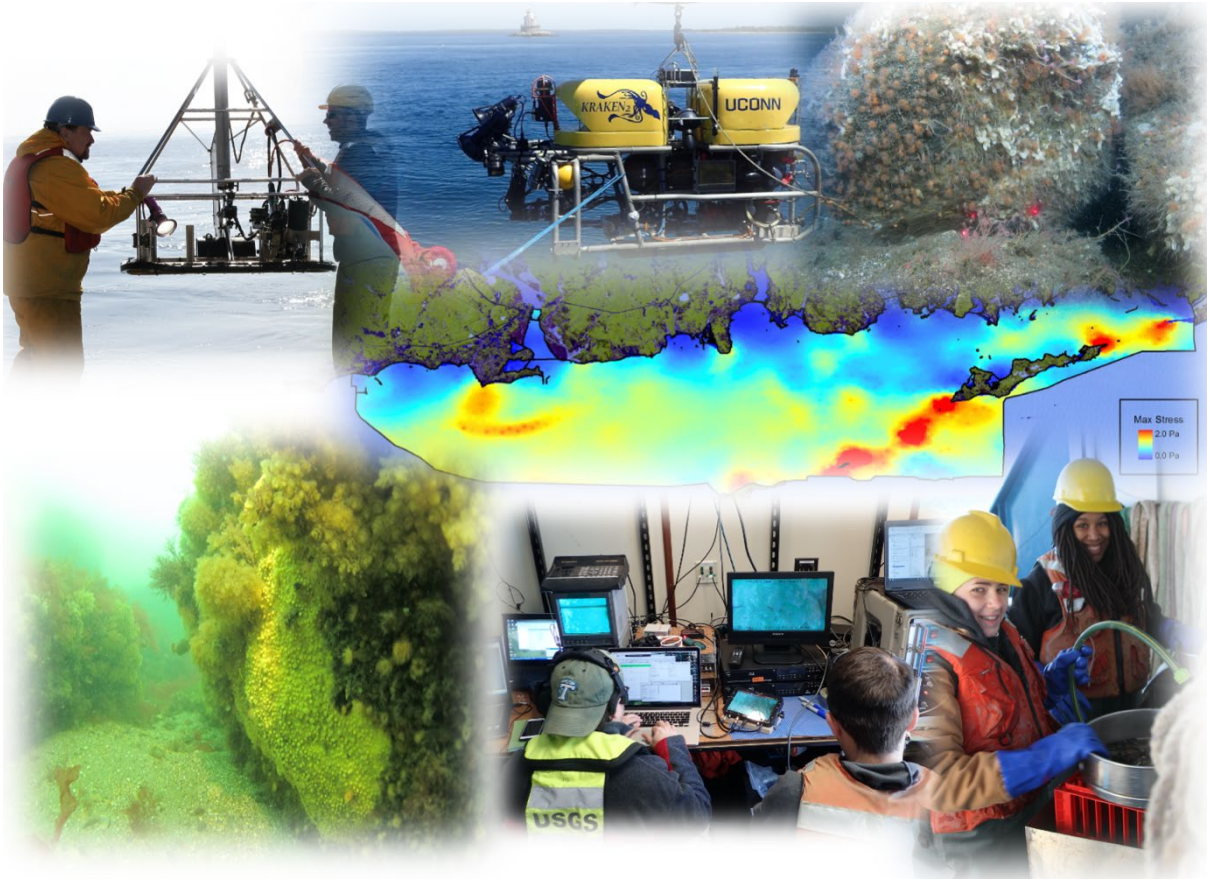

Final Report

Submitted by:
The Long Island Sound Mapping and Research Collaborative (LISMaRC)

August 23, 2021
Revised April 7, 2022

Long Island Sound Study
A Partnership to Restore and Protect the Sound

Connecticut Department of
ENERGY & ENVIRONMENTAL PROTECTION

4.0 SEA FLOOR / HABITAT CHARACTERIZATION

Recommended Citations:

Schneeburger, C. and Zajac, R. N. (2021). Historical Context. Section 4.1 in "Seafloor/Habitat Characterization" p. 47-50 in *The Long Island Sound Habitat Mapping Initiative Phase II – Eastern Long Island Sound – Final Report* (Unpublished project report).

Schneeburger, C. and Zajac, R. N. (2021). Methods. Section 4.1 in "Seafloor/Habitat Characterization" p. 51-53 in *The Long Island Sound Habitat Mapping Initiative Phase II – Eastern Long Island Sound – Final Report* (Unpublished project report).

Schneeburger, C. and Zajac, R. N. (2021). Results. Section 4.1 in "Seafloor/Habitat Characterization" p. 53-62 in *The Long Island Sound Habitat Mapping Initiative Phase II – Eastern Long Island Sound – Final Report* (Unpublished project report).

Schneeburger, C. and Zajac, R. N. (2021). Discussion. Section 4.1 in "Seafloor/Habitat Characterization" p. 63-64 in *The Long Island Sound Habitat Mapping Initiative Phase II – Eastern Long Island Sound – Final Report* (Unpublished project report).

Schneeburger, C. and Zajac, R. N. (2021). References. Section 4.1 in "Seafloor/Habitat Characterization" p. 64-65 in *The Long Island Sound Habitat Mapping Initiative Phase II – Eastern Long Island Sound – Final Report* (Unpublished project report).

4.1 Historical Context

Studies characterizing the geomorphology and sedimentary environments of the seafloor in LIS, as well as benthic ecological studies, have a history going back to the mid-1950s (Zajac, 1998). However, collectively the studies are spatially and temporally disjointed to various degrees, including the area encompassed by the Phase II study area. Early studies of sediment composition indicated that the Phase II study area was primarily comprised of sandy to coarse grained sediments with various mixtures of gravel, and in some shallow depths, small areas that also had sandy silts and clays (Figure 4.1-1). The spatial density, and as such resolution, of the sampling used to develop these initial sedimentary characterizations was low, and as such provided a spatially coarse understanding of sea floor environments (habitats) in this portion of LIS.

Poppe et al. (2000) complied data sets from a variety of studies conducted between the 1970s and 1990s and generated a more comprehensive characterization of the sediment distribution in LIS, including the whole of the Phase II study area (Figure 4.1-2). Their surficial sediment texture map revealed a spatially complex distribution of sedimentary patches of varying sizes comprised of primarily sand, gravelly sand, gravel/bedrock and to a lesser extent silty sand. A few patches of sand-silt-clay and sandy silt were identified in some shallow water areas along coasts and in harbors and bays. Poppe et al.'s (2000) map provides a large-scale depiction of the spatial distribution of general sediment /habitat types in the Phase II area. A related study by Knebel and Poppe (2000) showed that the sedimentary environment in the Phase II area is dominated by large areas of erosion or nondeposition and coarse-grained bedload transport (Figure 4.1-3), as well as geomorphological features such as sand wave and boulder fields.

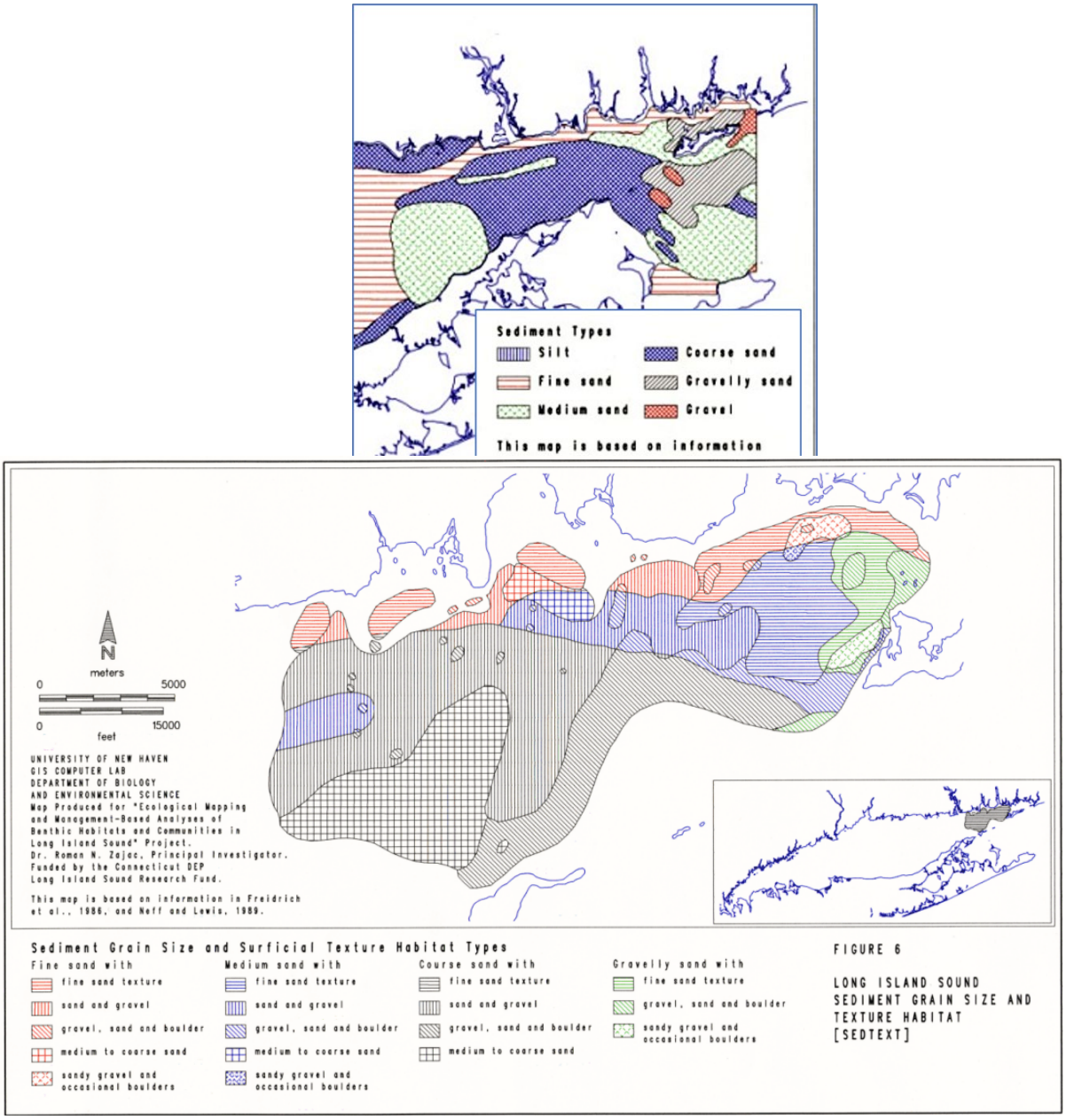

Figure 4.1-1 Examples of early sediment / habitat maps of the Phase II study area. Top: section of map from Freidrich et al. (1986) which reviewed and incorporated information from previous studies to develop a sediment grain-size distribution map. Bottom: Map developed by Zajac (1998) by combining information in Freidrich et al. (1986) and Neff and Lewis (1989) to delineate sedimentary habitats in eastern long Island Sound.

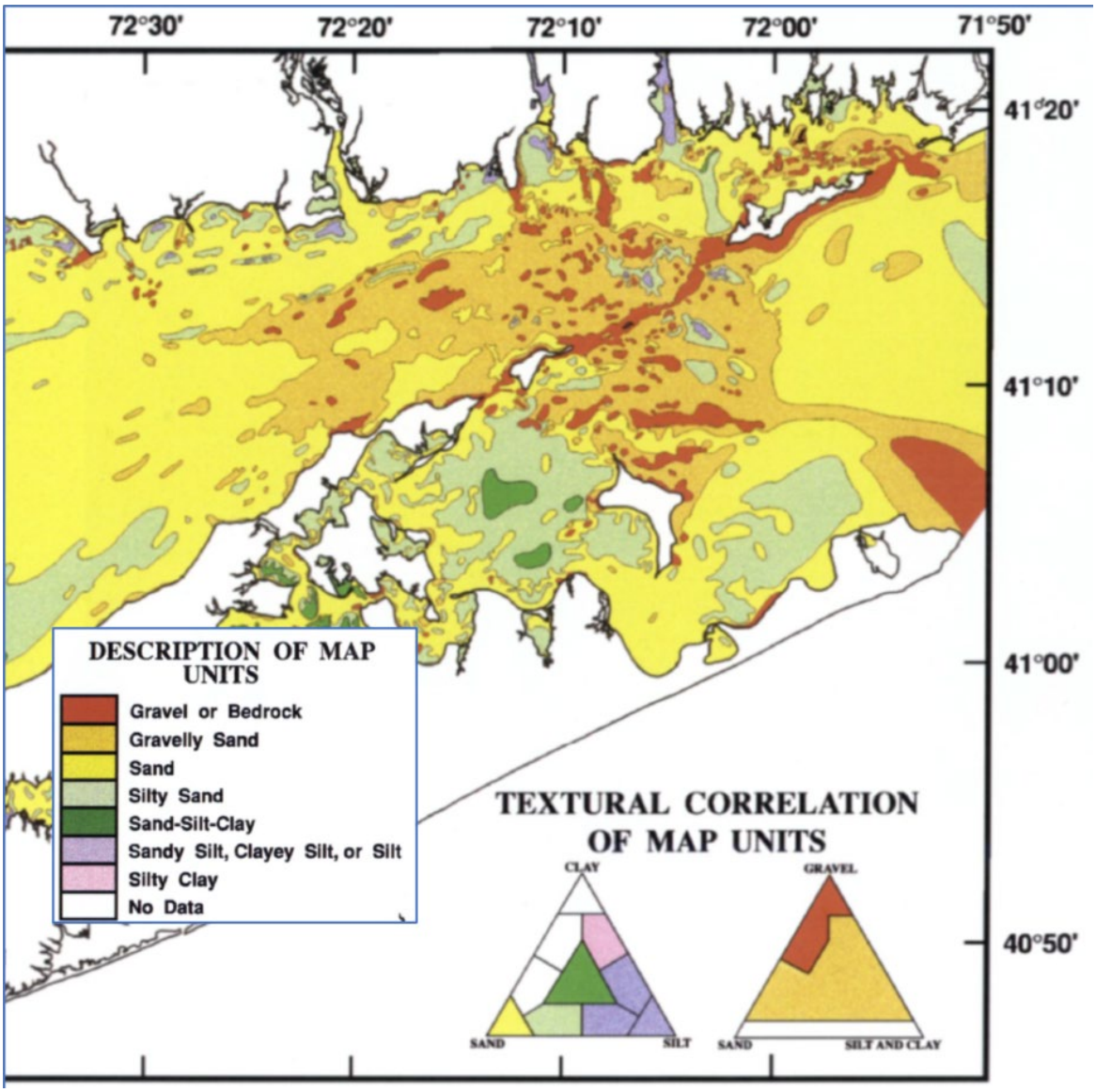

Figure 4.1-2 Portion of sedimentary texture map developed by Poppe et al. (2000) for Long Island Sound showing large-scale distribution of sediment types in the Phase II study area.

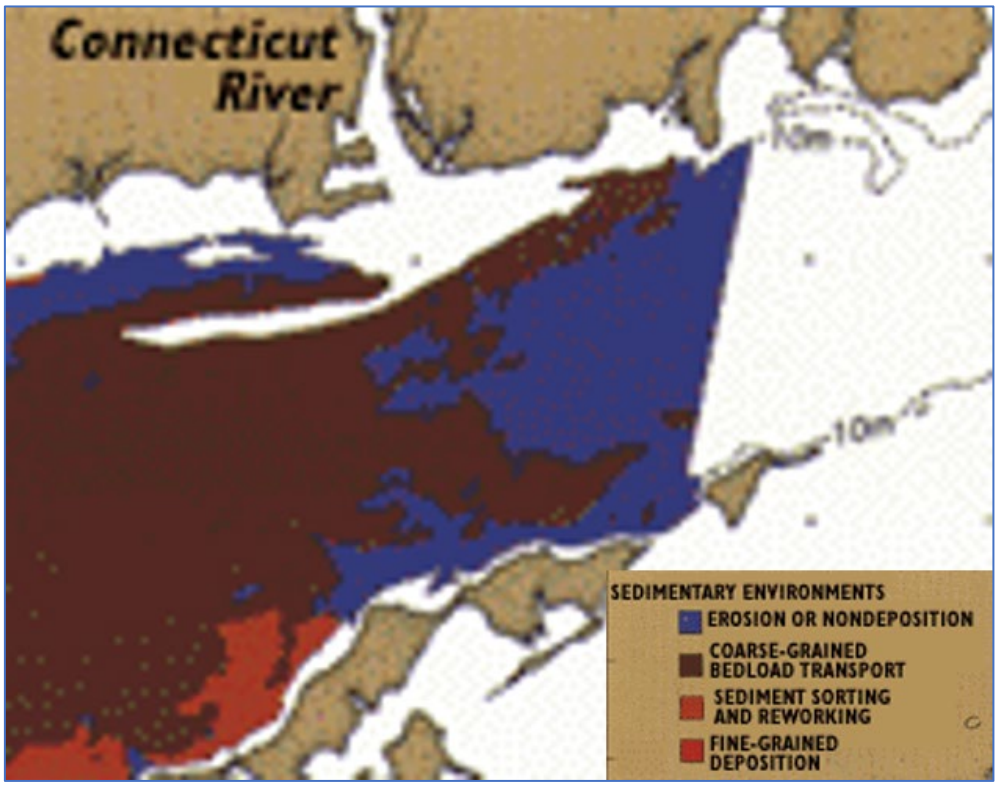

Figure 4.1-3 Sedimentary environments from Knebel and Poppe (2000) in a portion of the Phase II study area.

More spatially detailed studies of specific locations in the Phase II area revealed significant complexity to the sea floor landscape (or benthoscape) at smaller scales. For example, Zajac et al. (2000, 2003) studied a 19.4 km^2 area of the sea floor off the mouth of the Thames River, and found that within large-scale, general sediment-type patches interpreted from a side scan mosaic image, there was significant variation in sediment grain-size composition and biogenic and geomorphologic structural features. There have been several other studies of the sea floor in this region (see for example, https://coastalmap.marine.usgs.gov/regional/contusa/eastcoast/midatl/lis/data.html

Based on these previous studies, the Phase II study is highly dynamic in terms of sedimentary processes, has a complex geomorphology in some areas, and is dominated by primarily sandy and coarser grained sediments, which is supported by the seafloor characterization in the current study. Specific sediment composition and geomorphological characteristics can vary within patches of general sediment types (e.g., those indicated in Figure 4.1-2) and particularly across the many transition zones (e.g. Zajac et al., 2003) from one general sediment type to another that are present in the Phase II area (Figure 4.1-2), as local physical conditions vary across the region.

4.2 Methods

4.2.1 Data Sources Used for Seafloor Characterization

Several types of data representing different seafloor characteristics were used to classify and subsequently characterize the seafloor in the study area. These included a multibeam backscatter mosaic (Figure 4.2-1), bathymetry, seafloor rugosity as measured by the Terrain Roughness Index (TRI), maximum physical bottom stress, and sediment grain-size composition. The backscatter and bathymetric data and subsequent mosaic images created from the backscatter were collected by the National Oceanic and Atmospheric Administration (Batista et al. 2017). The spatial resolution of the backscatter was 2 m per pixel. The TRI for the study area was calculated by Conroy (2021 – this report) and the maximum bottom shear stress projections were developed by O'Donnell et al. (see Chapter 6 of this report). Sediment data at teach bottom sampling site was obtained and processed by the USGS (Ackerman et al., 2020).

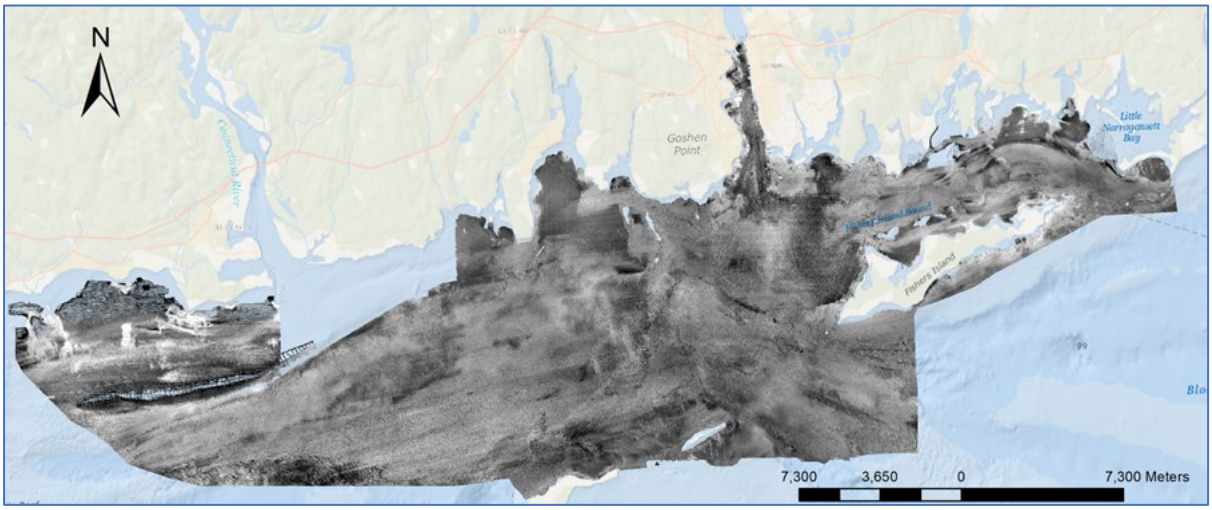

Figure 4.2-1 Acoustic backscatter mosaic of the Phase II study area that was used for seafloor characterization. Darker shades generally represent finer sediments; lighter shades generally represent coarser sediments.

4.2.2 Object-oriented Classification

The integrated backscatter mosaic of the seafloor of the pilot area was analyzed using eCognition Developer 9.4.0 (Trimble, 2019). This software segments the mosaic into meaningful objects (image-objects) of various sizes based on spectral and spatial characteristics (Lucieer, 2008) to perform a multi-segmentation classification to find regions with similar pixel values based on mean pixel brightness. The multiresolution segmentation criteria for this study were modeled based on previous studies on object-based seafloor image classification conducted by Lucieer (2008). Based on eCognition terminology, the mean brightness is equivalent to the mean intensity value of the backscatter pixels. The algorithm for multiresolution segmentation works by producing image objects based on pixel intensity to produce discrete objects that are homogeneous with respect to spectral characteristics (Drăguţ et al., 2010). The multiresolution segmentation was performed several times with different scale parameter segmentations to produce image objects that best represented the backscatter tones. A scale parameter value restricts the objects from becoming too heterogeneous (Trimble, 2019). A low parameter (near 0) would allow for higher heterogeneity and as the scale parameter increases, heterogeneity decreases. It was determined that a scale parameter of 100 worked best for the backscatter image of the Phase

II study area used in this analysis. A homogeneity criterion determines how spatially close the segments will be to one another and is comprised of shape and compactness. Several trials indicated that setting shape / smoothness to 0.9 and compactness to 0.6 were most effective for the backscatter image. The segmentation procedure resulted in an image that differentiated areas with similar pixel properties (Figure 4.2-2)

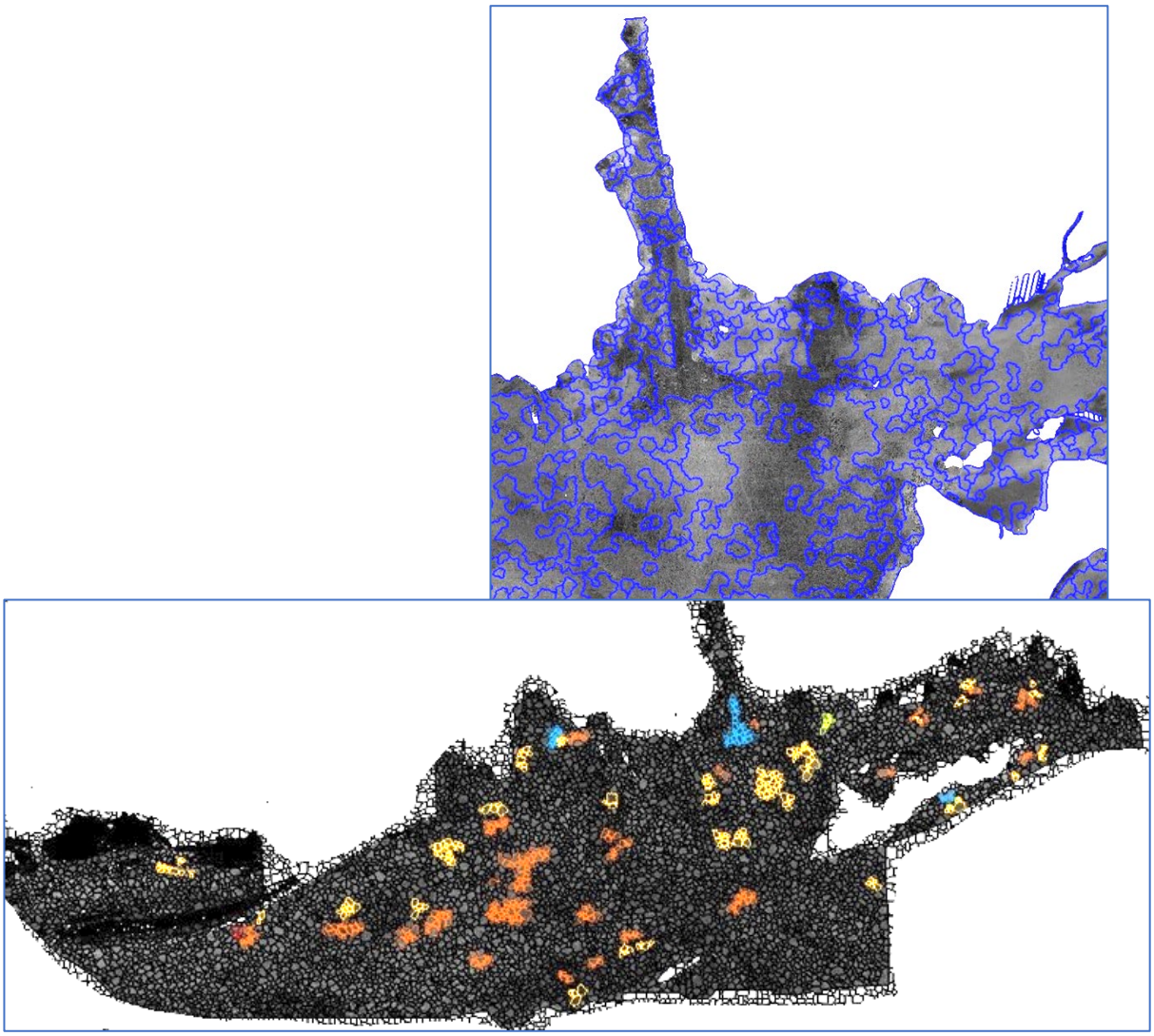

Figure 4.2-2 Examples of images segmentation and class sampling. Top: Results of image segmentation showing closeup around the mouth of the Thames River. Bottom: Sampling different segments to develop classification.

An unsupervised classification was then performed using eCognition by comparing the image objects with the underlying boundaries of pixel tone across the image. Five classes were designated based on general sedimentary groups (gravel, gravelly sediment, sand, silty sand, and sandy silt) used by the USGS for analysis of sediment samples obtained at the Phase II sampling sites (Ackerman et al., 2020). These classes were assigned initial image properties (mean and standard deviation of pixel intensities) by "sampling" visually distinct areas in the segmented backscatter mosaic (Figure 4.2-2). These properties were then adjusted as needed as well as setting nearest neighbor parameters that set how adjacent segments are merged into a specific class based on local homogeneity among neighboring segments and their image

properties or identified as being in different classes. The merging procedure produced 2,425 patches based on the image properties of the backscatter mosaic, and are referred to acoustic patches and assigned to the five, initial, sediment-based classes used in the classification / merging procedure. These acoustic patch types were then analyzed to assess their environmental characteristics and used as the basis for habitat identification and ecological characterization.

After the completion of object-oriented classification, the classified image was exported so that it could be integrated into GIS for further analyses. Using GIS, the classified image was imported as a shapefile and the classes assigned by eCognition were symbolized as separate acoustic patch types. The term acoustic patches refers to seafloor areas that have certain image characteristics (*i.e.*, a specific range of pixel intensities) based on acoustic backscatter data that are related to seafloor properties such sediment type and geomorphology, and were defined through a supervised image classification process. The acoustic patch types represent general habitat areas that have certain environmental characteristics with regard to sediment grain size composition, topographic roughness, and maximum hydrodynamic stresses on the seafloor. These characteristics are potential determinants of the kinds of infaunal and epifaunal communities that may be found within the acoustic patch types. The acoustic patch types can be designated as habitat types, and their mapped distribution forms the basis of an overall habitat map for the Phase II study area. This also forms the framework for subsequent research and surveys that can assess the accuracy of the characteristics of these habitat types as determined in this study and also the extent of the distribution of seafloor habitats in this portion of LIS.

This acoustic patch type data layer was then spatially joined with a file containing the sample points from the 2017 and 2018 surveys and the sediment data from the USGS. Patch analyst (Elkie et al.,1999) was used to run spatial statistics, and derive acoustic patch metrics (e.g. size and area). Sample points were joined with environmental data layers to extract data for bathymetry, TRI and bottom shear stress we All GIS analyses were conducted using ArcGIS 10.5.1. The data base was exported form GIS and used for univariate and multivariate statistical analyses using NCSS 11 (NCSS 2016) and PRIMER7 (Clarke and Gorley, 2015).

4.3 Results

The identified acoustic patches were distributed throughout the Phase II study area (Figure 4.3-1), although there are some generally geographical trends. The most extensive class is patch Type D, which was designated as gravelly sand (Table 4.3-1). It is found throughout the study project area, particularly in the central portion where there is a large continuous section of seafloor of this type. There are 411 patches of Type D, accounting for 45.1% of the study area. The second most extensive class is Type C, designated as sand. The largest areas of this patch type are found along the Connecticut coast, south of the Thames River and along the southern boarders of the project area. Acoustic patch Type C is comprised of 479 patches and makes up 41% of the study area. The three other classes A, B, and E cover smaller portions of the project area making up 0.86%, 11.3%, and 1.7% of the study area, respectively. Types A and E occur as small patches. Type A is classified as sandy silt and found scattered along the northern boundaries and in central areas of the study area. Type B is designated as silty sand, and found in the western section of the project study area and primarily along the coasts of Connecticut, Fishers Island and Long Island. Type E is classified as sandy gravel and patches are primarily found in the west central portion of the Phase II study area.

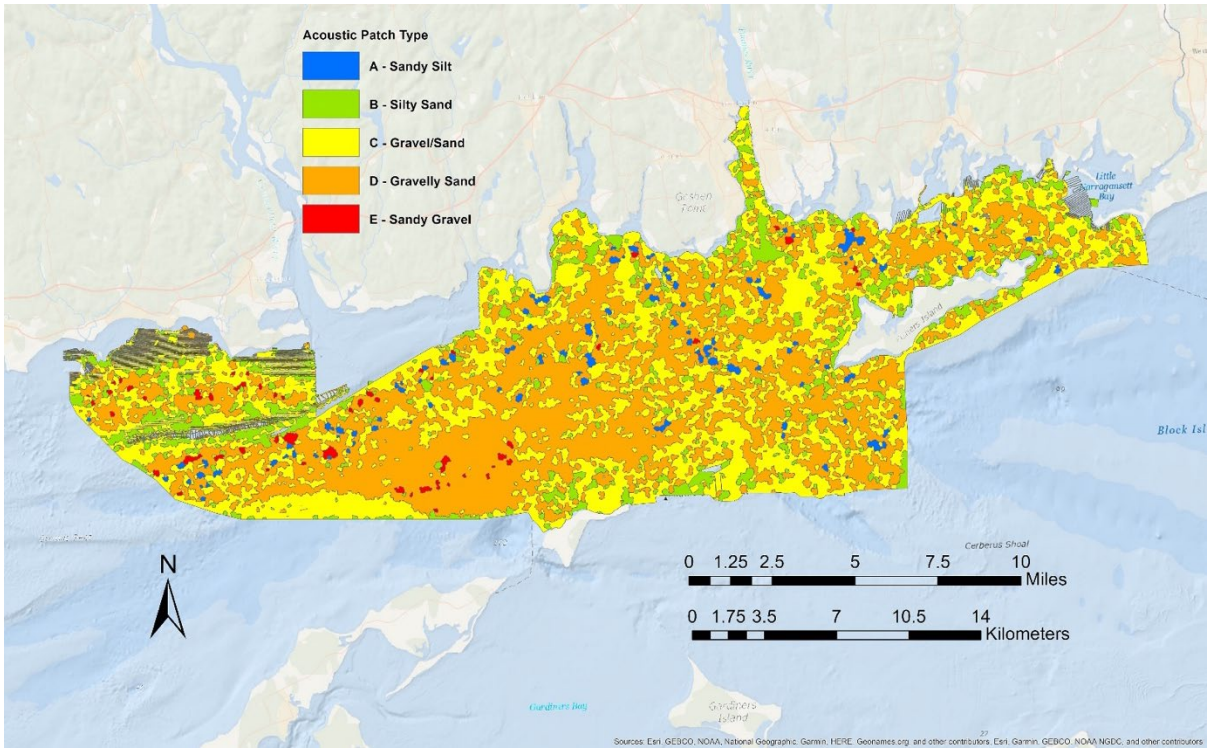

Figure 4.3-1 Acoustic patch types in the Phase II study area.

Table 4.3- 1. General characteristics of acoustic patch types identified in the Phase II study area. The number of samples from which sediment data is available is given as well as general sediment composition (% by weight) as determined by Ackerman et al

	Patch Type A	Patch Type B	Patch Type C	Patch Type D	Patch Type E
Total Area (ha) (% of total area)	780 (1.7%)	5,160.3 (11.3%)	18,650.1 (41%)	20,527 (45.1%)	391.7 (0.86%)
# Sediment Samples	1	15	71	81	1
Sediment class composition Mean % ± 1SE	G: 0.0 S: 35.3 Si: 45.5 C: 19.1	G: 6.6 ± 3.0 S: 82.3 ± 3.6 Si: 8.5 ± 2.5 C: 2.7 ± 0.8	G: 6.4 ± 1.4 S: 88.7 ± 1.6 Si: 3.5 ± 0.7 C: 1.3 ± 0.3	G: 19.9 ± 1.6 S: 75.4 ± 1.8 Si: 3.2 ± 0.7 C: 1.6 ± 0.6	G: 38.4 S: 61.1 Si: 0.4 C: 0.1
Depth Range (m)	8.9 - 9.1	4.95 - 86.8	5.39 - 95.01	6.0 - 89.48	30.54 - 48.0
Tidal Max Stress (Pascal) Range	0.451-0.461	0.191-2.685	0.221-2.052	0.214 - 1.864	0.938 - 0.997
TRI	0.013 -0.141	0.002 – 1.867	0.191 - 2.685	0.003 - 1.662	0.024 - 0.093

Although there were some broad geographical differences in spatial distribution of the acoustic patch types, the fact that each of the types were generally found in all areas of the Phase II study area, suggest that the environmental factors that determine their specific

characteristics are complex and interrelated. Over 85% of the Phase II study area is comprised of sandy sediment, and each acoustic patch type, except Type A, is characterized by over 65% sands by weight (Figure 4.3-2). Using a finer delineation of sediment grain-sizes based on a Phi scale, the acoustic patch types have different sediment compositions (Figure 4.3-3). Acoustic patch type A has the highest fraction of smaller grain sizes, dominated by silts and clays. Acoustic patch types B, C, D and E were dominated by sands, but have increasingly greater proportions of coarser grained sands and gravelly sediments, respectively. Patch types B, C and D had small amounts of silts and clays, whereas acoustic patch type E had almost no fine-grained sediments, but had the most gravel. Based on the sediment grain-size composition, the ND samples (which were not within the backscatter mosaic image area) are likely intermediate between patch type A and B, which is in line with these patch types being generally located in shallower waters (Figures 4.3-1 and 4.3-4). Patch types C, D and E were found in increasingly deeper waters, although there was great variation in depth for these patch types. Terrain roughness was relatively low for patch types A, E and the ND sample sites, and higher for types B, C and D (Fig. 4.3-5). Most notable, was the high variation in TRI for patch Types B, C, and D, indicating that for each of these patch types there are areas that have relatively large variations in local geomorphology, such as sand waves of different sizes and/or boulder fields. Maximum seabed stress increased in patch types A to C, respectively, and is highest in patch types D and E (Figure 4.3-6). As with TRI, bed stress is highly variable in patch types B, C and D.

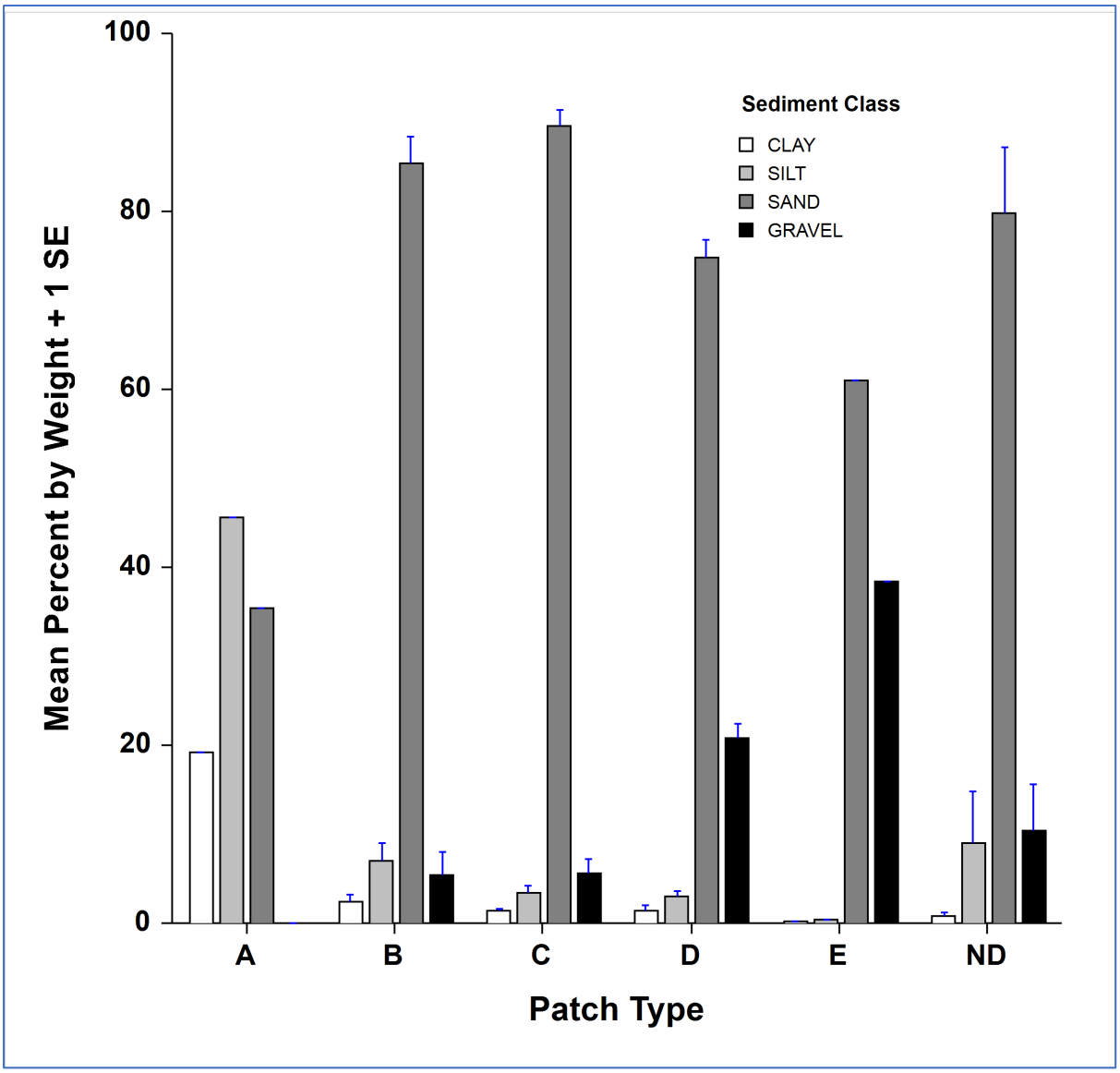

Figure 4.3-2 Mean percent composition (+1 standard error) of different sediment grain-size classes based on USGS classification (see Section 3.0)

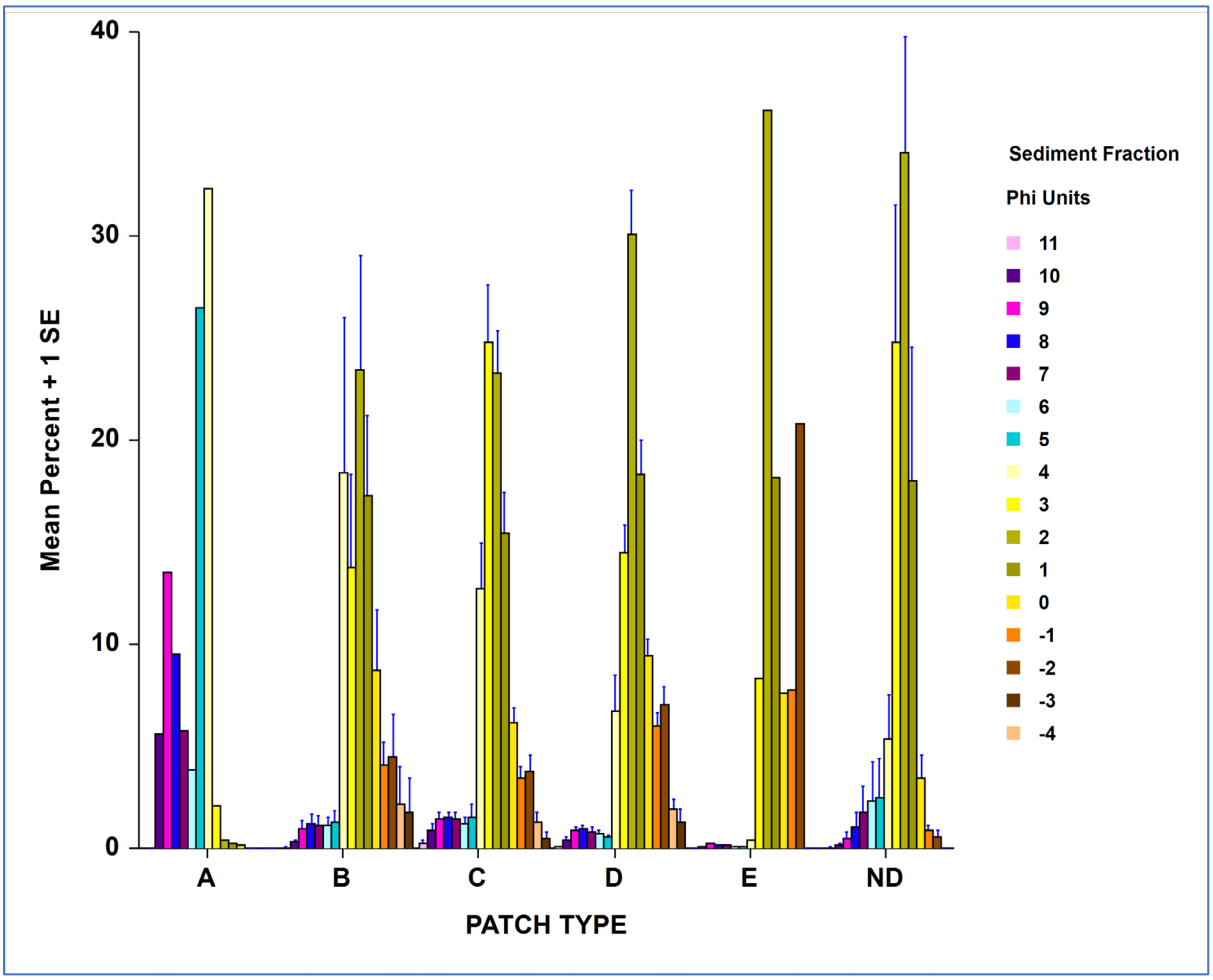

Figure 4.3-3 Sediment grain-size composition in the Acoustic Patch Types identified in the Phase II study area. ND = Not Determined, i.e., sites that were not in the backscatter mosaic image used to classify the patch types. Phi units range: clays, 11 to 8; silts, 8 to 4; sands, 4 to -1; gravels, -1 to -4. Lower phi values in each group indicate coarser sediments in that group. Sediment data was provided by the USGS (see Section 3.0 above).

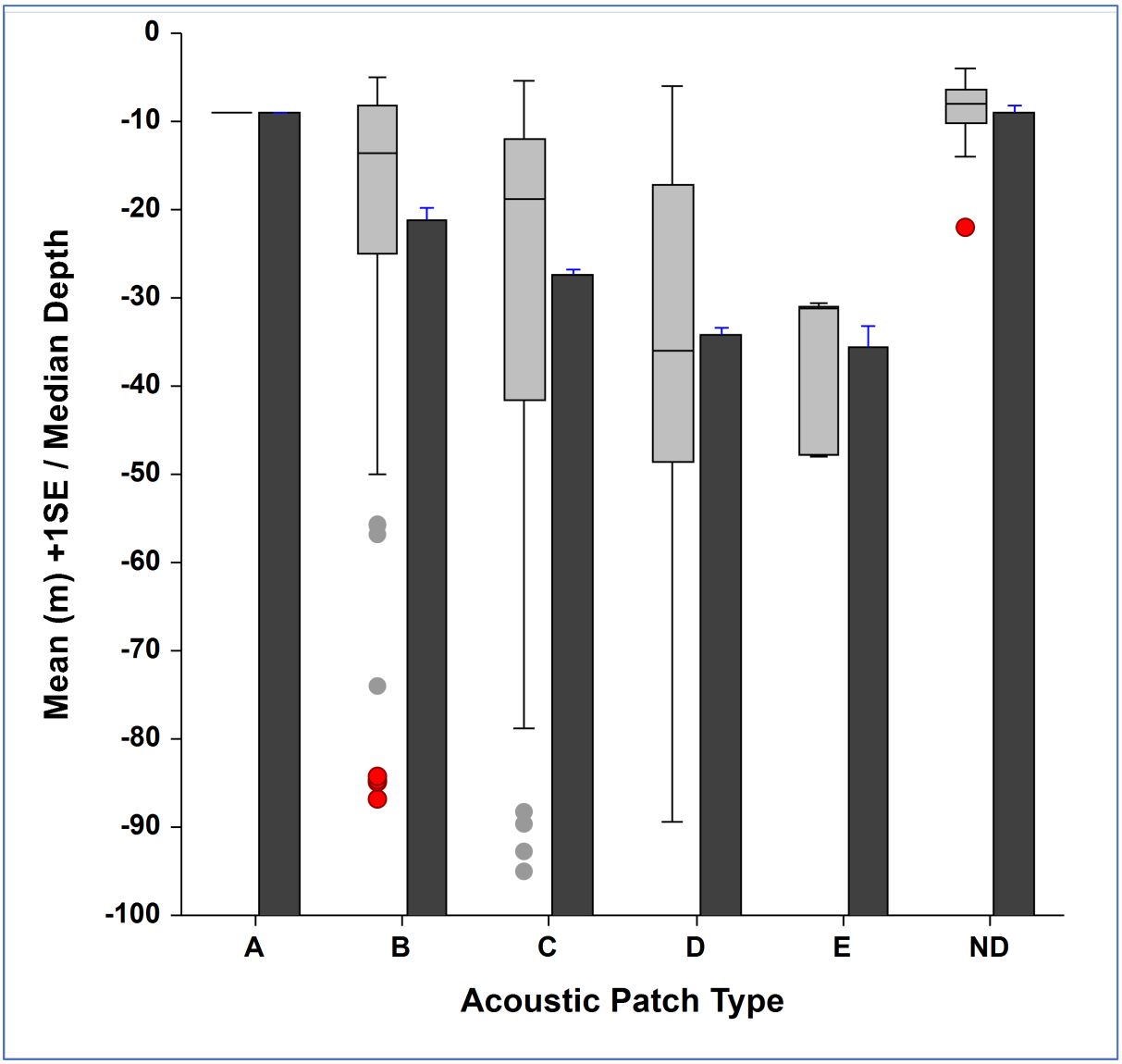

Figure 4.3-4 Depth characteristics of the acoustic patch types identified in the Phase II study area. ND = Not Determined, i.e., sites that were not in the backscatter mosaic image used to classify the patch types. Shown are the mean depth (+1 standard error, SE) and box plots showing the median (median ± 1.57 × (IQR) / √n), the inter-quartile range (IRQ) defined by the upper (75th percentile) and lower 25th percentile ends of the box, whiskers extending to 1.5 * IRQ. Outliers are shown as dots.

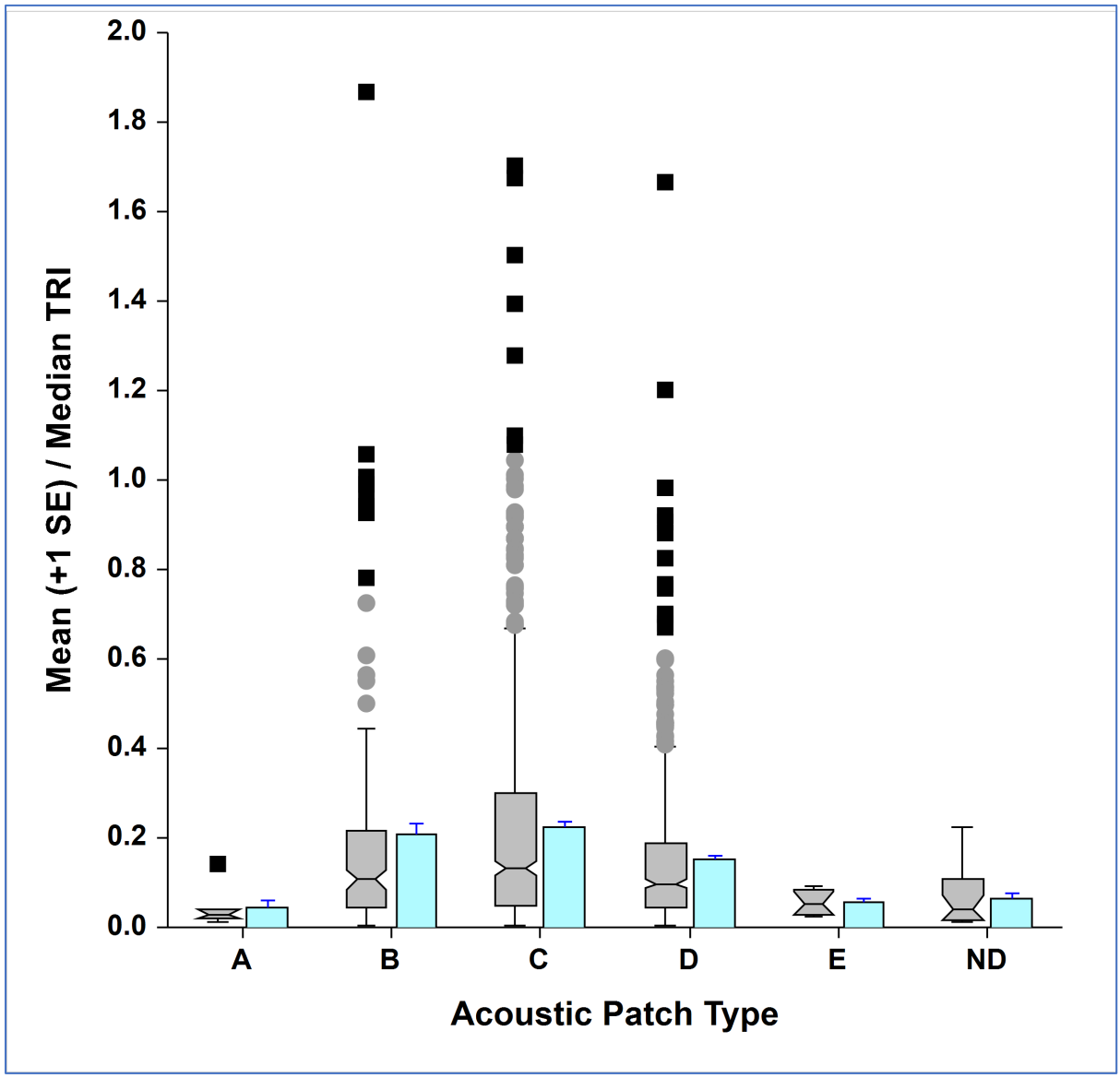

Figure 4.3-5 Terrain roughness (TRI) characteristics of the acoustic patch types identified in the Phase II study area. ND = Not Determined, i.e., sites that were not in the backscatter mosaic image used to classify the patch types. Shown are the mean depth (+1 standard error, SE) and box plots showing the notched median (median ± 1.57 × (IQR) / √n), the inter-quartile range (IRQ) defined by the upper (75th percentile) and lower 25th percentile ends of the box, whiskers extending to 1.5 * IRQ. Outliers are shown as dots.

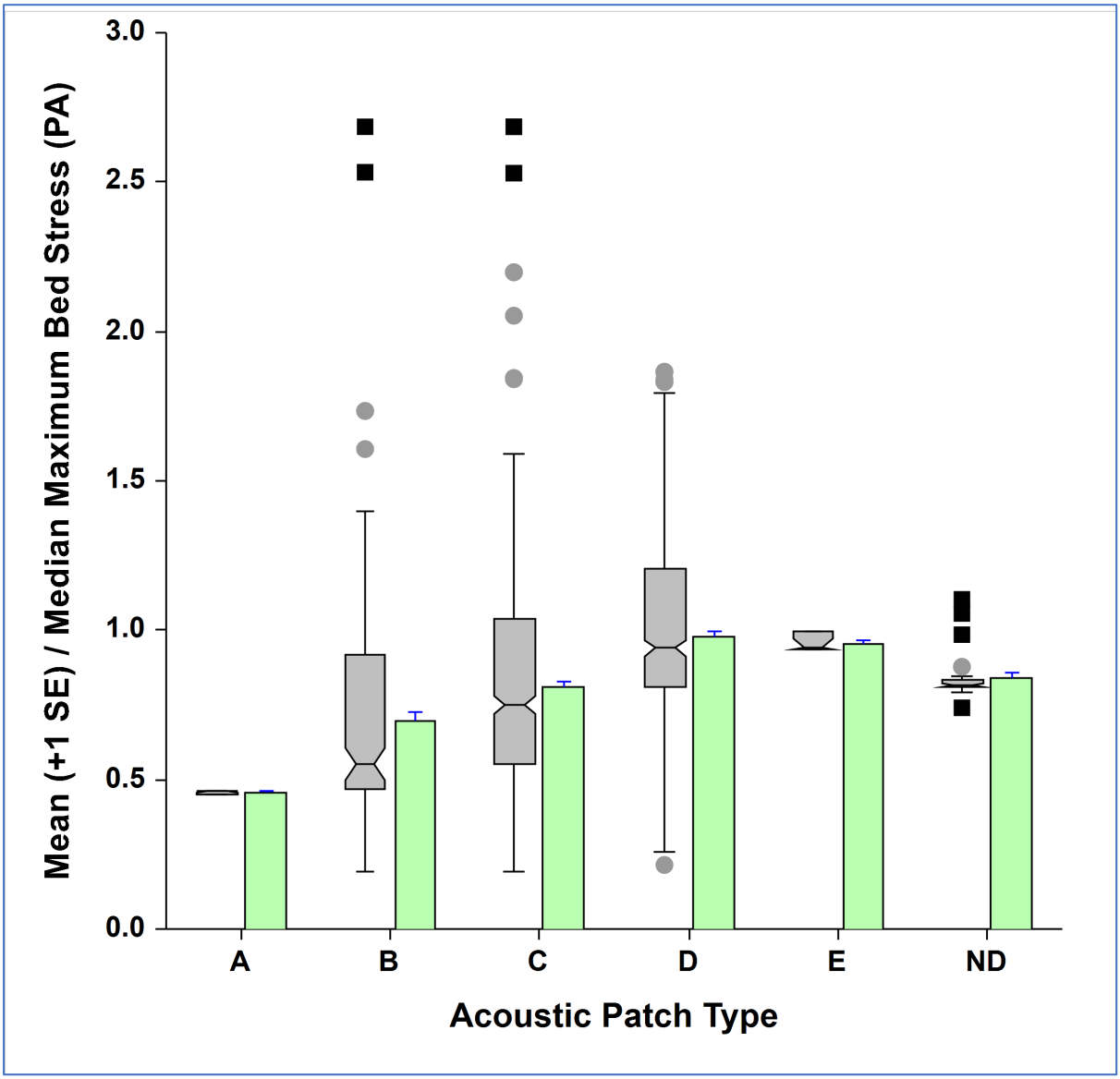

Figure 4.3-6 Maximum bed stress (PA=pascals) characteristics of the acoustic patch types identified in the Phase II study area. ND = Not Determined, i.e., sites that were not in the backscatter mosaic image used to classify the patch types. Shown are the mean depth (+1 standard error, SE) and box plots showing the notched median (median ± 1.57 × (IQR) / √n), the inter-quartile range (IRQ) defined by the upper (75th percentile) and lower 25th percentile ends of the box, whiskers extending to 1.5 * IRQ. Outliers are shown as dots.

Although the acoustic patch types are similar in that they are dominated by sandy sediments, multivariate analyses indicate that, based on all the environmental variables considered jointly, there are statistically significant differences with respect to their overall characteristics (Table 4.3-2). Pair-wise comparisons indicate that differences among patch Types A and B were marginally significantly, and significant differences exist among patch Types C and D, C and A, D and ND, and D and A. PCA ordination indicated that there was relatively high variability (dispersion) within patch Types B and C, and that most patch Type D samples were located closer together in the ordination space (Figure 4.3-7). Many of the Type C samples were separated from the other patch types due to being located in shallower depths and also containing higher proportions of sediments in the Phi 3 and 4 size-classes. Most of the patch type D sites were separated due to being in deeper waters and having coarser grain sizes and increasing maximum seabed stress. The gradient in sedimentary

differences and in the other environmental factors can be seen in the results of a CAP analysis (Figure 4.3-8). The ND and C patch types give way to patch Type D along the CAP2 axis, along a gradient from shallower depths and finer grain sizes to coarser grain sizes and to some extent increases in seabed stress and TRI.

Table 4.3- 2. Results of PERMANOVA analysis of differences among acoustic patch types relative to environmental factors (depth, TRI, maximum tidal stress and sedimentary phi classes). Data were normalized prior to generating a resemblance matrix using Euclidian distance. The analysis used a Type III (partial) sums of squares; fixed effects summed to zero for mixed terms; and 999 permutations of raw data.

PERMANOVA table of results

Source	df	SS	MS	Unique Pseudo-F	P(perm)
Patch Type	5	236.18	47.236	2.7603	0.003
Res	153	2618.2	17.113		
Total	158	2854.4			

Pair-wise tests (significant pairs are highlighted)

Groups	t	P(perm)
B, C	0.744	0.815
B, D	1.241	0.127
B, ND	1.072	0.290
B, E	0.664	0.745
B, A	1.958	0.062
C, D	1.931	0.001
C, ND	1.221	0.169
C, E	0.794	0.617
C, A	2.405	0.034
D, ND	1.930	0.004
D, E	0.652	0.738
D, A	2.971	0.018
ND, E	0.887	0.192
ND, A	2.241	0.190
E, A	No test	

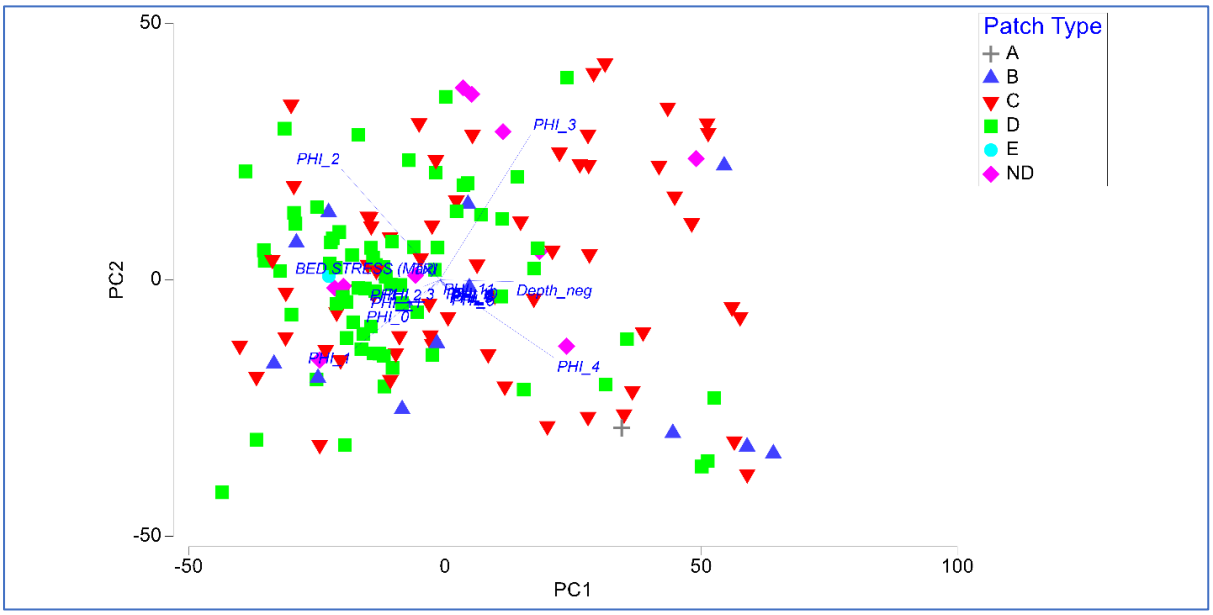

Figure 4.3-7 Principal Components Analysis (PCA) of sample sites in different acoustic patch types using sediment phi sizes, depth, maximum bed stress and TRI as variables. Vectors indicate the direction of separation of the sample sites due to the variables. Principal component axes 1 (PC1) and 2 (PC2) account 59.4 % of the total variation in the data.

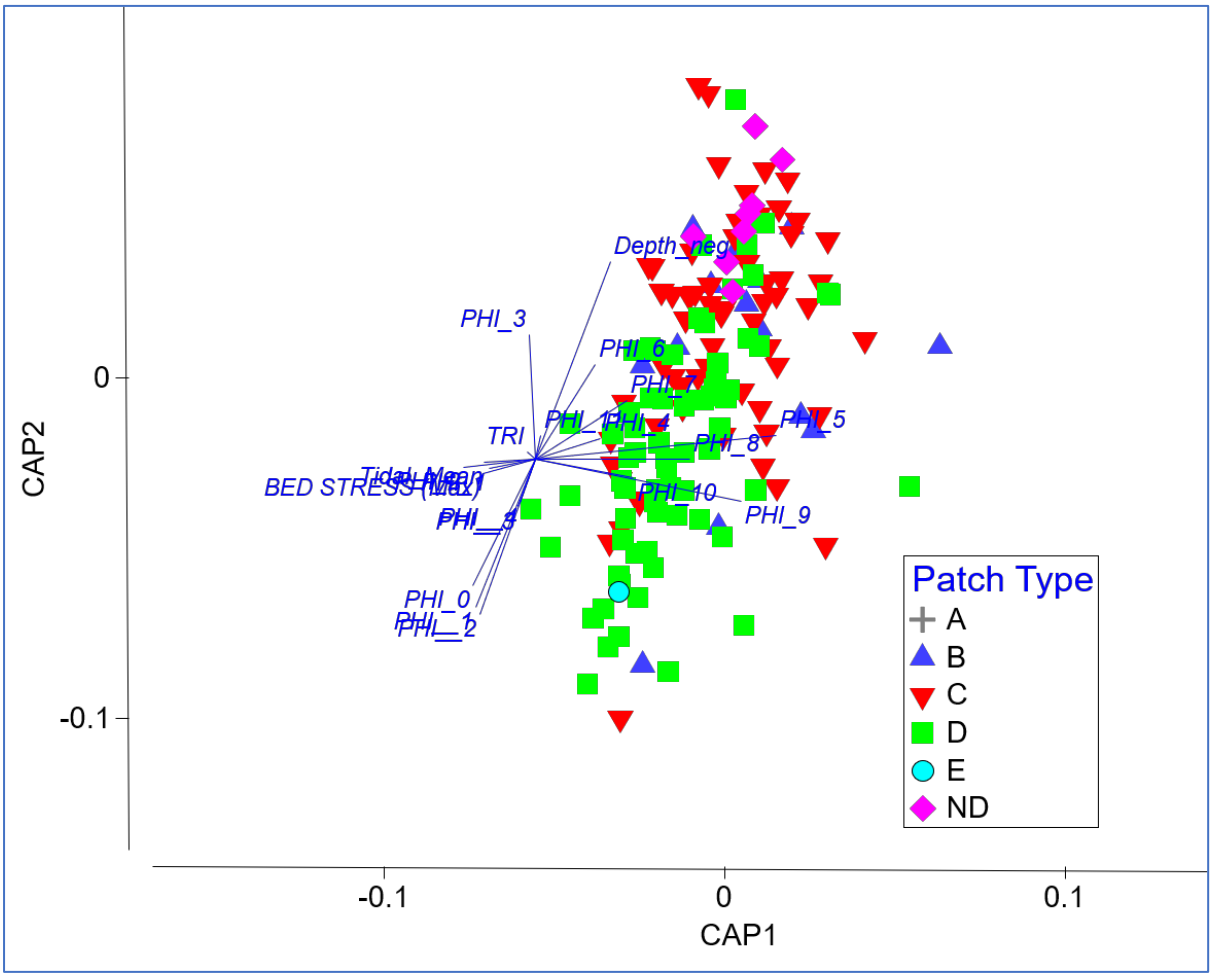

Figure 4.3-8 Results of canonical analysis of principal coordinates (CAP) to discriminate among acoustic patch types.

4.4 Discussion

Although sandy and gravelly sediments dominate 4 of the 5 acoustic patch types, there are distinct differences in the fine-scale composition of sediments in each acoustic patch type, representing a gradient from fine sands and silts to sand to sand/gravel from acoustic patch type A to E, respectively. The distribution of the patch types is spatially complex throughout most of the Phase II study area; however, some broader trends do emerge that are similar to previous mappings of sediment distributions in this portion of LIS. Both the sediment texture map (Figure 4.1-2) and the acoustic patch type map (Figure 4.3-1) indicate finer sediments along the Connecticut shore as well as closer inshore to Fishers Island, and to the north of Plum and Great Gull Islands. Both characterizations indicate a large area of gravelly sand in the central portion Phase II study area, extending from south of the Connecticut River to roughly South of Goshen Point, as well as in the central portions of Fishers Island Sound.

Likewise, both characterizations indicate a complex spatial distribution of patch types running north to south from the Connecticut shore to the area of the Race. One noticeable difference is that the sediment texture map (Figure 4.1-2) indicates a large band of bedrock/gravel extending from Plum Island to all along the southern shore of Fishers Island. The acoustic patch type characterization identifies these areas primarily as gravelly sand and a mix of gravel/sand and silty sand, particularly up against the Fishers Island south shore. This difference is likely due to extrapolations that were done for the sediment texture map and also the inability to collect samples in boulder areas using the sampling equipment for this project. There are boulder areas at a few of our sampling locations but these were not considered within the overall characterization, which was based solely on sediment composition, depth, maximum seabed stress, and topographic roughness. Increasing topographic roughness in patch types C, D and E indicate the presence of larger geomorphological features such as bedrock and boulder fields, as well as sand waves, in these patch types. For example, there are a number of relatively large sand wave fields in the Phase II area, particularly in the western portion (Figure 4.4-1). These sand wave fields increase TRI significantly in these areas and are primarily associated with acoustic patch types C and D, particularly the large field located along the southwest edge of the Phase II study area, which is almost entirely patch Type C.

The seafloor of the Phase II study area as represented by the acoustic patch types provides a framework for identifying benthic habitats and their spatial variation in this portion of LIS. The acoustic patches were identified using the image information in the acoustic backscatter data collected during multibeam surveys, and how that image data was compiled into the overall mosaic (Figure 4.2-1). The initial classification of bottom types was based on tonal differences in the backscatter mosaic. There are tonal differences across the mosaic that are not related to specific bottom type (e.g., in general, darker tones being finer sediments and letter tones being coarser sediments) due to striping where individual data segments were combined, shadowing, and also differences based on when the data was collected. In the segmentation process, differences in image tone across the mosaic may lead potential misclassification of certain areas in terms of one acoustic patch type or another. However, given the fact that much of the area is dominated by sandy sediments, the segmentation and delineation of acoustic patch types did differentiate among areas that had differing compositions of sand and gravel grain sizes. Additional analyses (not provided in this report) indicate that the sediment grain-size composition of each acoustic patch type was fairly consistent from east to west in the study area. The acoustic patch types thus represent general habitat areas that have certain environmental characteristics with regard to sediment grain

size composition, topographic roughness, and maximum hydrodynamic stresses on the seafloor. These characteristics are potential determinants of the kinds of infaunal and epifaunal communities that may be found within the acoustic patch types. However, other environmental and ecological factors can shape the ecological communities that may be present in the acoustic patch types. A more specific discussion of the link between the acoustic patch types and their ecological characteristics is provided in section 5.6.

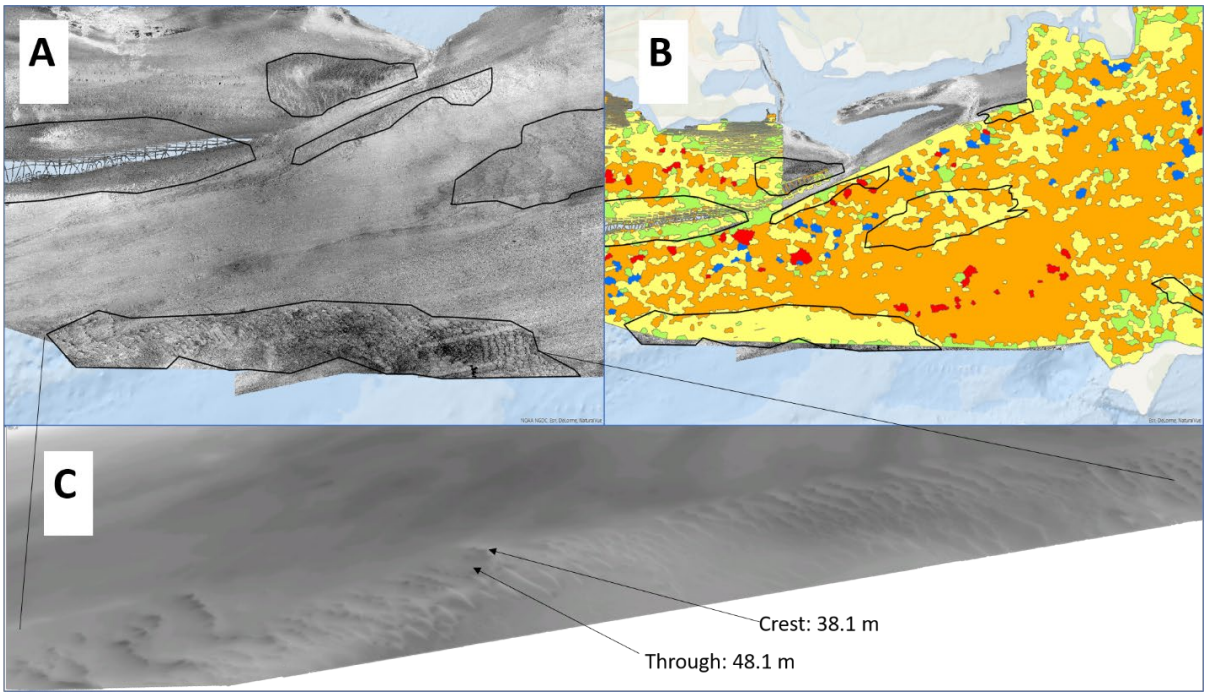

Figure 4.4-1 A: Location of several sand wave fields in the western portion of the Phase II study area. B: Areas of sand wave fields superimposed over acoustic patch types distribution (see Figure 4.6 for key for patch types. C: 3-D close-up of sand wave along the south-western edge of the Phase II study area; values represent depths at a representative crest and through within the sand wave field.

4.5 References - Seafloor Characterization

Ackerman, S.D., Huntley, E.C., Blackwood, D.S., Babb, I.G., Zajac, R.N., Conroy, C.W., Auster, P.J., Schneeberger, C.L., and Walton, O.L., (2020). *Sea-floor sediment and imagery data collected in Long Island Sound, Connecticut and New York, 2017 and 2018: U.S. Geological Survey data release.* https://doi.org/10.5066/P9GK29NM

Battista, T., W. Sautter, and R. Husted. (2017). *Bathymetry, acoustic backscatter, and LiDAR data collected in Long Island Sound for the Phase II Long Island Sound Seafloor Mapping Project 2015 (NCEI Accession 0167531).* NOAA National Centers for Environmental Information. Dataset.
https://www.ncei.noaa.gov/access/metadata/landing-page/bin/iso?id=gov.noaa.nodc:167531

Clarke, K.R. and Gorley, R.N. (2015). *PRIMER v7: User manual/tutorial*. PRIMER-E Plymouth.

Drăguţ, L.; Tiede, D.; Levick, S. (2010). ESP: a tool to estimate scale parameter for multiresolution image segmentation of remotely sensed data. *International Journal of Geographical Information Science.* Vol. 24(6), 859-871.

Elkie, P.C., Rempel. R.S. and Carr, A.P. (1999). *Patch Analyst Users Manual: A tool for quantifying landscape structure.* NWST technical manual TM-002. Ontario.

Freidrich, N.E., McMaster, R.L., Thomas, H.F., Lewis, R.S. (1986). *Non-energy Resources: Connecticut and Rhode Island Coastal Waters.* U.S. Dept. Interior, Minerals Management Service Cooperative Agreement No. 14-12-0001-30115, Final Report FY 1984.

Knebel, H.J. and Poppe, L.J., (2000). Sea-floor environments within Long Island Sound: a regional overview. *Journal of Coastal Research*, 16(3), 533-550.

Lucieer, V.L. 2008. Object-oriented classification of sidescan sonar data for mapping benthic marine habitats. *International Journal of Remote Sensing*. 29(3), 905-921.

NCSS 11 Statistical Software (2016). NCSS, LLC. Kaysville, Utah, USA, https://ncss.com/software/ncss

Neff, N.F., McMaster, R.L., Lewis, R.S., Thomas, H.F., (1988). *Non-energy resources: Connecticut and Rhode Island coastal waters.* U.S. Dept. Interior, Minerals Management Service Cooperative Agreement No. 14-12-0001-30316. Final Report FY 1986.

Poppe, L.J., Knebel, H.J., Mlodzinska, Z.J., Hastings, M.E. and Seekins, B.A., (2000). Distribution of surficial sediment in Long Island Sound and adjacent waters: texture and total organic carbon. *Journal of Coastal Research*. 16(3), 567-574

Trimble (2019). eCognition Developer 9.4.0 https://geospatial.trimble.com/products-and-solutions/ecognition

Zajac, R.N. (1998). A review of research on benthic communities conducted in Long Island Sound and an assessment of structure and dynamics. Chapter 4 in: *Long Island Sound Environmental Studies.* Poppe, L.J and Polloni, C. eds. https://pubs.usgs.gov/of/1998/of98-502/chapt4/rz1cont.htm

Zajac, R.N., Lewis, R.S., Poppe, L.J., Twichell, D.C., Vozarik, J. and DiGiacomo-Cohen, M.L., (2000). Relationships among sea-floor structure and benthic communities in Long Island Sound at regional and benthoscape scales. *Journal of Coastal Research*. 16(3), 627-640

Zajac, R.N., Lewis, R.S., Poppe, L.J., Twichell, D.C., Vozarik, J. and DiGiacomo-Cohen, M.L. (2003). Responses of infaunal populations to benthoscape structure and the potential importance of transition zones. *Limnology and Oceanography* 48, 829-842.